

Non-uniqueness and interpretation of the seawater $^{87}\text{Sr}/^{86}\text{Sr}$ curve

Dave Waltham^{a,*}, Darren R. Gröcke^b

^a *Department of Geology, Royal Holloway University of London, Egham, Surrey TW20 0EX, UK*

^b *School of Geography and Earth Sciences, McMaster University, 1280 Main Street, West Hamilton, Ont., Canada L8S 4K1*

Received 6 April 2005; accepted in revised form 14 September 2005

Abstract

Variations in the seawater $^{87}\text{Sr}/^{86}\text{Sr}$ curve through time can be caused by fluctuations in the strontium flux or variations in the isotopic ratio from at least six different sources and sinks. Thus, 12 or more parameters control each single measurement although widely accepted assumptions allow this to be reduced to typically six unknowns. Interpreting the causes of time-variation in the seawater $^{87}\text{Sr}/^{86}\text{Sr}$ curve is therefore hampered by inherent non-uniqueness. However, this problem is under-constrained rather than unconstrained. As a result, whilst there are an infinite number of possible interpretations, these all come from a few families of very similar solutions. Using this insight, it is possible to find solutions having the smallest possible variations in source flux or source $^{87}\text{Sr}/^{86}\text{Sr}$ ratio. Thus, lower-bounds can be placed upon the source variations responsible for the observed fluctuations in the seawater $^{87}\text{Sr}/^{86}\text{Sr}$ curve. When applied to the evolution of the Early Jurassic $^{87}\text{Sr}/^{86}\text{Sr}$ seawater curve, this approach demonstrates that a short-lived Toarcian event is genuine since it is present in all models, regardless of the values chosen for the unknown source fluxes and unknown source isotope ratios. However, the variations in strontium flux or isotopic ratio necessary to explain the Toarcian event may be significantly smaller than would be predicted assuming modern values for the unknown parameters.

© 2005 Elsevier Inc. All rights reserved.

1. Introduction

Interpretation of the variation in the seawater strontium isotope ratio with time is important in many studies of the ancient Earth system (e.g., Brass, 1976; Hodell et al., 1989, 1990, 1991; Berner and Rye, 1992; Françoise and Walker, 1992; Veizer et al., 1997, 1999; Pálffy and Smith, 2000; Jones and Jenkyns, 2001; Wallmann, 2001). However, a fundamental difficulty is that this ratio is controlled by a large number of time-varying factors and so a unique interpretation is not possible. However, it is not true to say that this problem is completely unconstrained. Although, there are an infinite number of ways to interpret the data, all solutions have properties in common and, as we show in this paper, it is possible to find the minimum variation in any given parameter that could have produced the observed seawater strontium isotope curve.

The application of strontium isotope ($^{87}\text{Sr}/^{86}\text{Sr}$) stratigraphy to the geological record has been extensive. Most of these studies have focused on the more recent past, particularly the Cenozoic (DePaolo and Ingram, 1985; Koepnick et al., 1985; Palmer and Elderfield, 1985; Clemens et al., 1993; Sugarman et al., 1997; Martin et al., 1999). However, over the past decade many studies have looked in particular at the Cretaceous period (McArthur et al., 1992, 1993, 1994; McLaughlin et al., 1995; Jenkyns et al., 1995; Bralower et al., 1997; Crame et al., 1999), which has been made possible with the recovery of well-preserved carbonate and microfossils from ODP cores. An increasing number of studies recently have been aimed at constructing the Jurassic portion of this curve (Koepnick et al., 1990; Jones, 1992; Jones et al., 1994a,b; Podlaha et al., 1998; McArthur et al., 2000; Hesselbo et al., 2002; Jenkyns et al., 2002; Price and Gröcke, 2002; Gröcke et al., 2003; Hall et al., 2004).

The seawater $^{87}\text{Sr}/^{86}\text{Sr}$ curve has therefore been reasonably well reconstructed but interpretation of the results is hampered by non-uniqueness, i.e., there is more than one

* Corresponding author.

E-mail addresses: d.waltham@gl.rhul.ac.uk (D. Waltham), grocke@mcmaster.ca (D.R. Gröcke).

sequence of events capable of reproducing the observed isotope variations. The under-determined nature of this problem is well illustrated by [Françoise and Walker \(1992\)](#) who discuss six different sources and sinks for strontium, namely:

1. Weathering of old igneous rocks ($^{87}\text{Sr}/^{86}\text{Sr} \sim 0.718$).
2. Weathering of young igneous rocks ($^{87}\text{Sr}/^{86}\text{Sr} \sim 0.705$).
3. Weathering of sedimentary rocks ($^{87}\text{Sr}/^{86}\text{Sr} \sim 0.708$).
4. Fluid exchange between the ocean and seafloor hydrothermal systems ($^{87}\text{Sr}/^{86}\text{Sr} \sim 0.703$).
5. Alteration of buried sediments by diagenetic fluids and expulsion of these into the oceans ($^{87}\text{Sr}/^{86}\text{Sr} \sim 0.708$).
6. Incorporation of oceanic strontium into carbonate sediments.

Each of these sources and sinks has an associated time-varying flux and time-varying isotope ratio and hence, for each moment in time, there are at least a dozen unknown factors and only a single measurement (i.e., the palaeo-seawater $^{87}\text{Sr}/^{86}\text{Sr}$ value).

There are several possible strategies for resolving this difficulty although none are completely satisfactory:

1. Many of the individual fluxes can be grouped together into a single flux. In particular, many authors group all of the weathering fluxes into a single riverine flux with a time-varying $^{87}\text{Sr}/^{86}\text{Sr}$ value controlled by the relative contributions of the three weathering-related sources (e.g., [Palmer and Elderfield, 1985](#); [Françoise and Walker, 1992](#); [Jones and Jenkyns, 2001](#)). We will also use this tactic in this paper.
2. The strontium isotope system can be assumed to be close to equilibrium at all times ([Hodell et al., 1989](#); [Berner and Rye, 1992](#)). This implies that the sources and sinks balance, i.e., there is an additional constraint. In this paper, we will assume that a balance between sources and sinks occurs but only when fluxes are averaged over time periods long compared to the strontium residence time in the oceans. Thus, we allow the system to be out of equilibrium on short time scales.
3. Some of the unknown parameters can be linked to other, hopefully better-constrained processes, for example the weathering rate (and hence, the riverine flux) can be related to atmospheric CO_2 concentrations (e.g., [Françoise and Walker, 1992](#); [Wallmann, 2001](#)). Although this is a very useful strategy, we will not use similar constraints here.
4. Educated guesses can be made concerning some of the unknown parameters, for example, present-day values can be assumed ([Hodell et al., 1990](#)). Alternatively, a number of solutions can be produced using educated guesses about likely ranges of controlling parameters ([Jones and Jenkyns, 2001](#)). We adopt a similar strategy in this paper except that we aim to investigate all possible solutions given such ranges rather than just a few examples.

These assumptions restrict the range of solutions but leave an infinite number of solutions within that range. The key new factor in our approach is that we find an approximate general form for all possible solutions to the problem. It is then a simple matter to find a specific solution having the smallest possible parameter variation with time. Thus, we can calculate lower-bounds for the time-variations in fluxes and/or isotope ratios. In addition, because we know how all solutions are related to each other, we can confidently extend conclusions based upon a single solution to the set of all solutions. In other words, this is mathematically much more rigorous than the frequently used approach of guessing reasonable values for the unknown parameters and then hoping, without real justification, that firm conclusions can be extrapolated from this one case (or even a limited range of cases).

2. The Early Jurassic seawater strontium isotope curve

The dataset we use ([Fig. 1](#)) is based upon a compilation given by [Jenkyns et al. \(2002\)](#). The stratigraphic resolution of these data is generally better than one ammonite subzone (i.e., about 200 kyr) and, in places, is constrained by intense sampling of belemnites giving it a resolution as high as 40 kyr. However, [McArthur et al. \(2000\)](#) have suggested that portions of the curve may have significantly greater time uncertainties, perhaps as great as 0.25 Myr.

In this paper, we concentrate upon a specific event in the Jurassic, namely a sharp rise in the seawater $^{87}\text{Sr}/^{86}\text{Sr}$ value at around 182 Ma. This rise has been discussed by [Pálffy and Smith \(2000\)](#) who note that it coincides with the emplacement of a large igneous province in Gondwana (Ferrar–Karoo). This event coincides with a minor extinction event and the global distribution of organic-rich black shales associated with the Toarcian oceanic anoxic event (see [Jenkyns et al., 2002](#)). [Pálffy and Smith \(2000\)](#) explain these events through an abrupt and short-lived increase in weathering rate resulting from volcanically enhanced greenhouse warming. However, it is possible that the observed rise in the $^{87}\text{Sr}/^{86}\text{Sr}$ curve results from long-term, gradual changes in conditions rather than from a short, sharp event. The methods developed here allow us to put lower-bounds, on the change in weathering rates, etc., necessary to produce the observed rise in the $^{87}\text{Sr}/^{86}\text{Sr}$ curve thus allowing us to eliminate this “null hypothesis.”

3. Preprocessing of the data

The application of strontium isotope ($^{87}\text{Sr}/^{86}\text{Sr}$) stratigraphy to the geological record becomes more straightforward if a representative smooth curve is constructed through the raw data. Many different methods can be used to generate such a curve (e.g., [LOWESS](#), [McArthur et al. \(2001\)](#)), but the smooth curve in [Fig. 1](#) was generated by fitting a linear regression through successive groups of 29 points (i.e., 14 points either side of a central point).

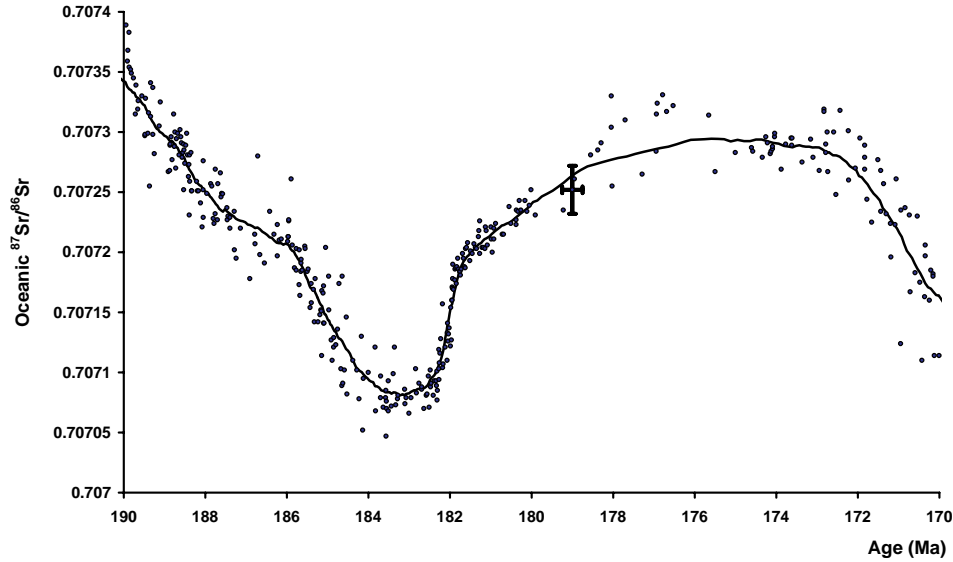


Fig. 1. Variation in the Early Jurassic seawater $^{87}\text{Sr}/^{86}\text{Sr}$ ratio (after Jenkyns et al., 2002). The error bars show estimated data uncertainties drawn through one of the points. The solid line shows a fit to the data which is used for the analysis in this paper.

The height of the regression line at the mean age of the 29 points then gives one point on the required smoothed curve. It should be noted that our data set extends considerably either side of the data plotted in Fig. 1 and so there are no edge problems with this approach. This regression approach also automatically generates a gradient for each averaged age (Fig. 2) and this curve is vital for the analysis that follows. Alternate techniques for obtaining a smoothed seawater $^{87}\text{Sr}/^{86}\text{Sr}$ curve would produce very similar results.

Whatever technique is used, the resulting smoothed curve should differ from the data by amounts that are comparable with the expected measurement errors. The root mean square error (rmse) between the curve in Fig. 1 and the data is 1.98×10^{-5} , which is comparable to the expected

accuracy of around 10^{-5} for individual measurements of $^{87}\text{Sr}/^{86}\text{Sr}$ (McArthur et al., 2001). The length of the smoothing operator should also be such that it does not remove real features from the data. Large changes in seawater $^{87}\text{Sr}/^{86}\text{Sr}$ values cannot occur on time scales short compared to the strontium residence time (i.e., a few million years) and the average width of the 29-point groups in this smoothed curve (~ 0.87 Myr) is significantly less than this. The conclusions from the analysis which follows are not substantially altered if the filter-length is changed unless it is either so short that the $\text{rmse} < 10^{-5}$ or so long that it removes features varying on time scales > 1 Myr. For comparison, one of the data points in Fig. 1 has conservative error bars attached (assumed to be 2×10^{-5} for the isotope ratios and 0.25 Myr for the ages).

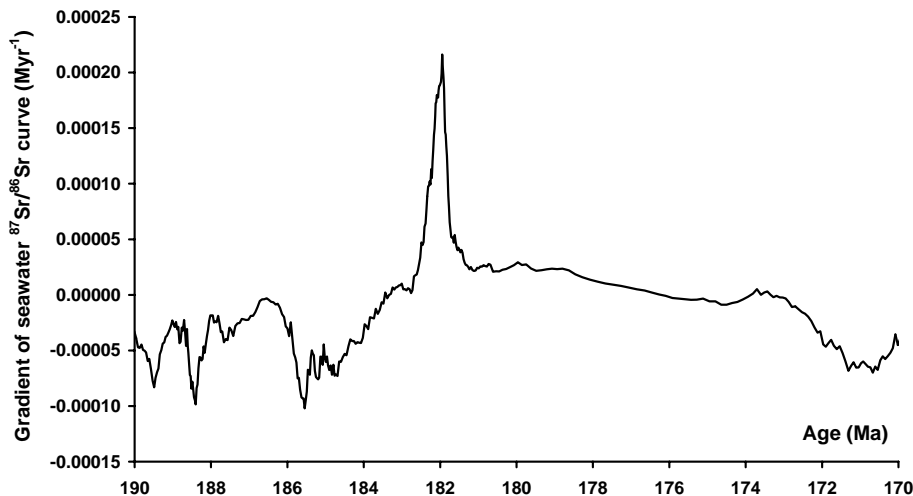


Fig. 2. Time derivative of curve in Fig. 1. The prominent spike around 182 Ma is the Toarcian event investigated in this paper.

4. The forward model

In this paper, we use the model of Hodell et al. (1989) and McCauley and DePaolo (1997), i.e.,

$$M\dot{R} = \sum_i (R_i - R)F_i, \quad (1)$$

where M is the total mass of strontium in the oceans, R is the strontium isotope ratio of the oceans, \dot{R} is time derivative of R , R_i is the isotope ratio of a source or sink, and F_i is the corresponding flux. We also follow the lead of Françoise and Walker (1992) and consider four distinct fluxes, i.e., a burial flux, a continental weathering flux, a hydrothermal flux, and a diagenetic flux.

The unknown total mass, M , can be removed from Eq. (1) by making the assumption that

$$F_0 = -M/\tau, \quad (2)$$

where F_0 is the burial flux and τ is the residence time (Jones and Jenkyns, 2001). Eq. (1) can then be rewritten as

$$\tau\dot{R} = \sum_i (R_i - R)f_i, \quad (3)$$

where f_i is the i th flux expressed as a fraction of the burial flux (i.e., $f_i = -F_i/F_0$). It should be noted that the burial flux only changes significantly on time scales greater than the order of τ . Hence, if a short-lived event (i.e., lasting less than τ) is due to variations in a normalized flux, f_i , the implication is that it is caused specifically by variations in the associated flux, F_i , rather than by variations in F_0 .

The next step is to note that the isotope ratio in the burial flux is identical to that in seawater and so $(R_0 - R) = 0$ and the corresponding term disappears from Eq. (3) to give

$$\tau\dot{R} = f_w(R_w - R) + f_h(R_h - R) + f_d(R_d - R) \quad (4)$$

with subscripts w, h, and d indicating weathering sources, hydrothermal sources, and diagenetic sources, respectively. Note that τ , R , f_w , R_w , f_h , R_h , f_d , and R_d can all vary with time and so we have one equation and seven unknowns (R is known since it is the observed seawater $^{87}\text{Sr}/^{86}\text{Sr}$ curve).

The analysis presented in this paper requires an additional assumption, which can be illustrated using Fig. 2. The most prominent feature, and the one concentrated upon in this paper, is a strong spike lasting ~ 1 Myr that is centred at 182 Ma. This spike corresponds to a sharp increase in $^{87}\text{Sr}/^{86}\text{Sr}$ values at this time as shown in Fig. 1. We assume, in the following, that this event is due to variation in a single factor. This assumption ignores correlations but these will be discussed later in this paper. It should also be noted that the size of this spike is sensitive to dating errors and that McArthur et al. (2000) have suggested that this portion of the seawater $^{87}\text{Sr}/^{86}\text{Sr}$ curve may be significantly condensed. We tackle this difficulty, later in the paper, by assuming that the calculated peak gradient in Fig. 2 (i.e., 0.00022 Myr^{-1}) may be exaggerated by as much as a factor of 2.

Given these caveats, we look at two distinct types of explanation for the observed time-variation in the seawater $^{87}\text{Sr}/^{86}\text{Sr}$ curve:

- (1) The spike was caused by a sharp change in the flux from one of the sources. For example, if it resulted from a change in the continental weathering flux, then $f_w = f_w(t)$ whilst τ , R_w , f_h , R_h , f_d , and R_d are unknown constants.
- (2) The spike was caused by a sharp change in the strontium isotope ratio from one of the sources. For example, if the $^{87}\text{Sr}/^{86}\text{Sr}$ ratio from continental weathering changed then $R_w = R_w(t)$ whilst τ , f_w , f_h , R_h , f_d , and R_d are unknown constants.

There is one final possibility that encapsulates one of the major points of this paper. It is quite possible for smoothly changing parameters to give rise, at certain critical times, to dramatic changes in the character of the seawater $^{87}\text{Sr}/^{86}\text{Sr}$ ratio. Fig. 3 illustrates this using the forward model of Eq. (4). All parameters were assumed to have constant values, except for the weathering flux, f_w , which was assumed to be increasing at a steady rate of 0.01 Myr^{-1} . Note that this model shows an initial decline in seawater $^{87}\text{Sr}/^{86}\text{Sr}$ followed by a rise and has similar behaviour to the true seawater $^{87}\text{Sr}/^{86}\text{Sr}$ curve between 186 and 181 Ma. Hence, it may be that there is nothing unusual happening at all at around 182 Ma and the sharp rise in the seawater $^{87}\text{Sr}/^{86}\text{Sr}$ ratio simply results from the interaction of smoothly changing parameters that happen to pass threshold values at this point in time. Circumstances such as this are almost bound to occur, by chance, during the 500 Myr period for which we have reliable $^{87}\text{Sr}/^{86}\text{Sr}$ data. Thus, a major objective of this paper is to eliminate the possibility that the behaviour of the $^{87}\text{Sr}/^{86}\text{Sr}$ curve at 182 Ma results from smoothly changing parameters rather than being caused by a distinct event.

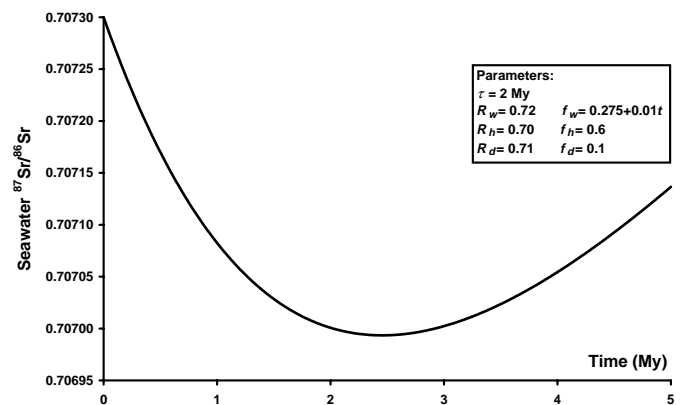


Fig. 3. Forward model using Eq. (4) and the parameters indicated. Note that all parameters are constant except for the weathering flux which is increasing at a constant rate. Nevertheless, an inflection occurs in the predicted seawater $^{87}\text{Sr}/^{86}\text{Sr}$ curve.

5. The inverse model

5.1. Time-averaged fluxes and isotope ratios

Before considering time-variation in the fluxes or $^{87}\text{Sr}/^{86}\text{Sr}$ ratios from each of the sources, it is useful to first look at constraints on their time-averaged values. There are three key approximations used throughout the remainder of this paper which produce such constraints. First, the variation in the seawater $^{87}\text{Sr}/^{86}\text{Sr}$ ratio is very small compared to its mean value (relative standard deviation (RSD) = 0.0001 for our data) and so R can be replaced by \bar{R} in Eq. (4) without much loss of accuracy. Note that over-bars indicate time-averaging throughout this paper. Second, the variation in the time derivative, \dot{R} , is large compared to its mean (RSD = 10) and so $\dot{R} \approx 0$ is also a good approximation. Third, the sources fluxes should balance the burial flux over time-periods long compared to τ and so $\bar{f}_w + \bar{f}_h + \bar{f}_d = 1$.

$$(5)$$

These three approximations, together with the assumption that short-term variations in seawater $^{87}\text{Sr}/^{86}\text{Sr}$ ratio are caused by variation in a single flux or source isotope ratio, allow Eq. (4) to be time averaged and simplified to give

$$\bar{f}_w \bar{R}_w + \bar{f}_h \bar{R}_h + \bar{f}_d \bar{R}_d \approx \bar{R}. \quad (6)$$

A further constraint arises because the diagenetic source involves fluids migrating through sediments which will dominantly have been deposited a relatively short time previously. The modern diagenetic $^{87}\text{Sr}/^{86}\text{Sr}$ value (0.7084, from Jones and Jenkyns, 2001) is well approximated by the average oceanic $^{87}\text{Sr}/^{86}\text{Sr}$ ratio over the last 35 Myr (McArthur et al., 2001) and we assume that the same was true in the Jurassic so that

$$\bar{R}_d \approx \bar{R}. \quad (7)$$

Eqs. (5)–(7) give three equations in six unknowns and so three unknowns must be specified before they can be solved. We start by assuming that the diagenetic flux was similar to today's, i.e., $\bar{f}_d \sim 0.07$ (Jones and Jenkyns, 2001). This flux is small and so the effects of it being incorrectly guessed are relatively minor. We also assume that the hydrothermal source $^{87}\text{Sr}/^{86}\text{Sr}$ ratio is close to today's with $\bar{R}_h \sim 0.7033$ (Palmer and Edmond, 1989). Finally, we assume that the $^{87}\text{Sr}/^{86}\text{Sr}$ ratio from continental weathering was slightly smaller in the Jurassic than today (because modern values are significantly enhanced by the effects of Himalayan erosion) and had a value of $\bar{R}_w \sim 0.7100$.

Given assumed values for these parameters, Eqs. (5)–(7) yield

$$\bar{f}_w \approx \frac{(1 - \bar{f}_d)(\bar{R} - \bar{R}_h)}{\bar{R}_w - \bar{R}_h} \quad (8)$$

and

$$\bar{f}_h \approx \frac{(1 - \bar{f}_d)(\bar{R}_w - \bar{R})}{\bar{R}_w - \bar{R}_h}. \quad (9)$$

For our best-guess parameters these give $\bar{f}_w = 0.543$ and $\bar{f}_h = 0.387$.

Given these expressions, it is possible to investigate how these time-averaged fluxes are affected by differing assumptions for the unknown constants. The mean weathering source flux, for example, is very sensitive to \bar{R}_w but only weakly sensitive to \bar{R}_h and \bar{f}_d . Fig. 4 shows these dependencies. It is interesting to note that the Jurassic seawater $^{87}\text{Sr}/^{86}\text{Sr}$ curve is incompatible with the estimates of modern weathering flux and modern weathering $^{87}\text{Sr}/^{86}\text{Sr}$ ratio. Assuming that the Jurassic flux and Jurassic ratio are as similar as possible to their modern values suggests $\bar{f}_w \sim 0.5$ and $\bar{R}_w \sim 0.710$ as assumed in our best-guess scenario.

All best-guess parameters are summarized in Table 1, which also has our best-guess residence time (τ 2.4 Myr from Jones and Jenkyns, 2001) and our best-guess at the maximum rate of change in the seawater $^{87}\text{Sr}/^{86}\text{Sr}$ curve during the studied period ($\dot{R}_{\text{max}} \sim 0.00022 \text{ Myr}^{-1}$, taken from the 182 Ma peak in Fig. 2). These additional parameters will be used below.

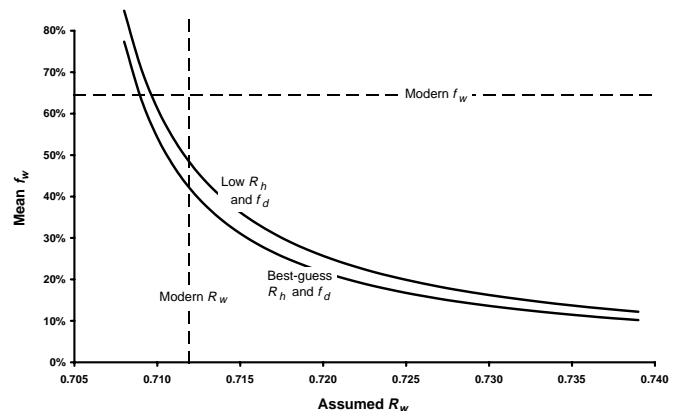


Fig. 4. Time-averaged weathering flux predicted by Eq. (8). Note, this is most sensitive to the choice of time-averaged weathering source $^{87}\text{Sr}/^{86}\text{Sr}$ ratio.

Table 1
Time-averaged values of parameters used in modelling

	Best-guess	Extreme
τ (Myr)	2.4	1.0
\bar{R}_w	0.7100	0.7384
\bar{R}_h	0.7033	0.7028
\bar{R}_d	0.7072	0.7072
\bar{f}_w	54%	12%
\bar{f}_h	39%	88%
\bar{f}_d	7%	0%
\bar{R}	0.7072	0.7072
\dot{R} (max)	0.00022	0.00011

Note that \bar{f}_w and \bar{f}_h have been calculated from Eqs. (8) and (9) using the other assumed parameter values. \bar{R} and \dot{R} (max) have been determined from the Early Jurassic seawater $^{87}\text{Sr}/^{86}\text{Sr}$ curve (i.e., Fig. 1).

5.2. Time-varying fluxes

With this background, we can now look at the flux and isotope ratio fluctuations necessary to give the observed seawater $^{87}\text{Sr}/^{86}\text{Sr}$ curve. If it is assumed that the evolution of the seawater $^{87}\text{Sr}/^{86}\text{Sr}$ curve was caused only by time-variation in the continental weathering flux then, from Eq. (4)

$$f_w = [\tau\dot{R} - f_h(R_h - R) - f_d(R_d - R)]/(R_w - R), \quad (10)$$

where all symbols on the right-hand side are constants, except for R and \dot{R} . Using our best-guess values for the unknown τ , f_h , R_h , f_d , R_d , and R_w (Table 1) gives the Early Jurassic weathering flux shown in Fig. 5. The key feature is a short, sharp spike at 182 Ma indicating that the rise in the seawater $^{87}\text{Sr}/^{86}\text{Sr}$ curve at this time could be explained by a short-lived increase in the flux of strontium from continental weathering. With these parameters, the weathering flux had a mean equal to 55% of the burial flux and this increased by 17% during this brief episode. However, given that there are six unknown constants in Eq. (5), it is far from clear whether all possible solutions have a similar spike and, if they do, how the spike size is affected by changes in the parameters.

To answer this question, it is useful to recast Eq. (10) in terms of its deviation from the mean, i.e., $\Delta f_w = f_w - \bar{f}_w$. Using the approximations $R \approx \bar{R}$ and $\dot{R} \approx 0$, Eq. (10) yields the remarkably simple result that

$$\Delta f_w \approx \frac{-\tau\dot{R}}{R_w - \bar{R}}. \quad (11)$$

Substitution of the best-guess values from Table 1 into this expression gives a maximum deviation from the mean of 19%, in reasonable agreement with the value found from direct use of Eq. (10). Eqs (8) and (11) can be combined to give a weathering flux ratio versus time curve and this is shown in Fig. 5 for comparison with that obtained using Eq. (10). Note that the two curves are reasonably similar

thus supporting the validity of the approximations made in deriving Eqs. (8) and (11). However, it should be emphasized that, when inverting for $f_w(t)$, Eq. (10) should be used since this is the more accurate expression.

The importance of Eqs. (8) and (11) lies in their ability to show how results are altered by changed assumptions rather than in the fact that they also give an estimate of $f_w(t)$. In particular, Eq. (11) yields two very important results. First, all $f_w(t)$ curves will have deviations from the mean which are well approximated by scaled versions of the time-derivative curve shown in Fig. 2. All models will therefore have a peak at 182 Ma and there will be no choices for τ , f_h , R_h , f_d , R_d , and R_w which remove the 182 Ma event. Second, the event will be smallest when τ and \dot{R} are minimized whilst R_w is maximized.

Extreme values for our controlling parameters are given in Table 1. Oslick et al. (1994) is the source for our lowest residence time ($\tau \sim 1$ Myr) whilst the lower-limit to \dot{R} was obtained simply by assuming that the data around 182 Ma in Fig. 1 may have been condensed by up to a factor of 2 thus doubling the peak gradient. Our maximum-allowed weathering source $^{87}\text{Sr}/^{86}\text{Sr}$ ratio assumed that its global-mean value was close to the maximum observed from any single modern source (Palmer and Edmond, 1989). Thus, using these extreme values from Table 1 gives the result that the changes in the seawater strontium isotope ratio curve at 182 Ma can, in principle, be accounted for by an increase in the weathering flux equal to a mere 0.3% of the burial flux.

However, this result is particularly sensitive to the value of R_w and Fig. 6 shows how this affects the maximum deviation assuming all other parameters are fixed. In reality, R_w is unlikely to be higher than its modern value since the effects of Himalayan erosion probably elevate this above typical values. Therefore, a more realistic lower-limit for this event is that it required an increase in weathering flux equivalent to 2% of the burial flux.

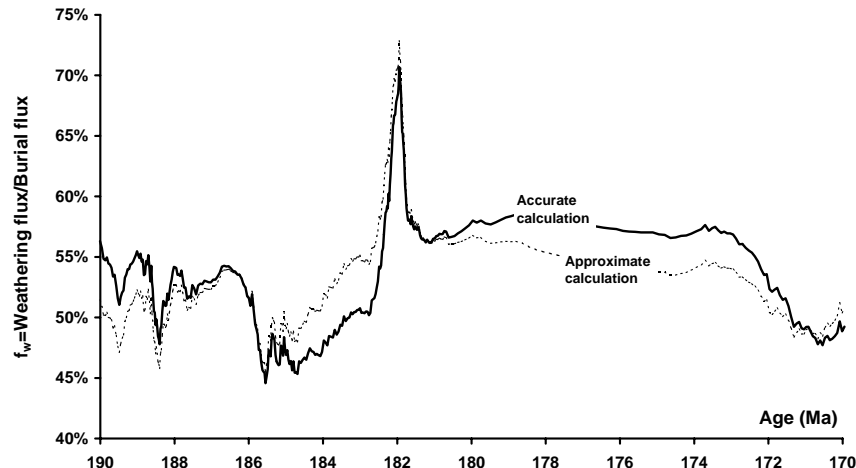


Fig. 5. Normalized weathering flux, f_w , as a function of time. The accurate calculation comes from Eq. (10) whilst the approximate calculation comes from Eqs (8) and (11). All constants come from the best-guess column of Table 1.

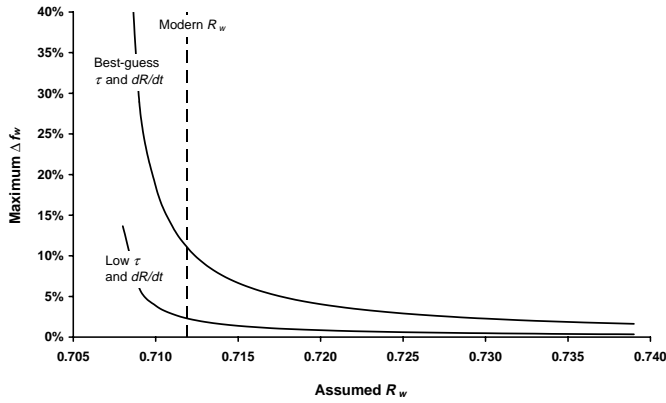


Fig. 6. Deviation from the time-averaged weathering flux at the peak of the 182 Ma event. The upper curve assumes best-guess values from Table 1 whilst the lower curve uses the extreme values in the same table. Note that the deviation is expressed as a fraction of the burial flux.

A similar approach to that used above can be employed to investigating time-varying diagenetic or hydrothermal fluxes. The general result is that, if the variation in the seawater $^{87}\text{Sr}/^{86}\text{Sr}$ curve results from time-variation in a single flux, the deviation from the mean is well approximated by

$$\Delta f_x \approx \frac{\tau \dot{R}}{R_x - \bar{R}}, \quad (12)$$

where x is w , h or d .

This provides insight into the variations in the hydrothermal or diagenetic systems necessary to give the observed variations in the seawater $^{87}\text{Sr}/^{86}\text{Sr}$ curve. The hydrothermal source $^{87}\text{Sr}/^{86}\text{Sr}$ ratio is about 0.004 less than the mean seawater $^{87}\text{Sr}/^{86}\text{Sr}$ ratio (cf. the weathering source $^{87}\text{Sr}/^{86}\text{Sr}$ ratio is about 0.003 higher than seawater) and so the necessary fluctuations in hydrothermal flux are similar in size, but opposite in sign, to those discussed for the

weathering flux. Hence, the 182 Ma event can be explained by a short, sharp reduction in hydrothermal flux of the order of 1.5–15% of the burial flux. This seems feasible except that it is hard to imagine a mechanism which produces a short, sharp reduction in hydrothermal strontium flux.

Diagenetic sources, on the other hand, have very similar $^{87}\text{Sr}/^{86}\text{Sr}$ ratios to that of seawater and Eq. (12) therefore implies flux-variations which are an order of magnitude or more greater than those required for the weathering-flux-variation or hydrothermal-flux-variation explanations. Hence, the 182 Ma event is very unlikely to have been caused by variations in the flux of diagenetic fluids beneath the seafloor.

5.3. Time-varying isotope ratios

The second type of model capable of explaining the observed behaviour in the seawater $^{87}\text{Sr}/^{86}\text{Sr}$ at around 182 Ma is one in which the $^{87}\text{Sr}/^{86}\text{Sr}$ value from one of the sources is varying through time. For example, if we assume that the global mean $^{87}\text{Sr}/^{86}\text{Sr}$ value in river water, resulting from weathering of the continents, is varying through time then Eq. (4) gives

$$R_w = R + \frac{\tau \dot{R}}{f_w} - \frac{f_h}{f_w} (R_h - R) - \frac{f_d}{f_w} (R_d - R) \quad (13)$$

in which $R_w = R_w(t)$, $R = R(t)$, and $\dot{R} = \dot{R}(t)$ whilst all other symbols are, unknown, constants. Using best-guess estimates (Table 1) for the unknown constants then gives the curve shown in Fig. 7. This shows a clear peak in the isotope ratio, at around 182 Ma, which is 0.0009 above the mean of 0.7100.

We now need to know how this peak alters as the unknown parameters are changed. Making the same approximations as before (i.e., $R \approx \bar{R}$, $\dot{R} \approx 0$, and $R_d \approx \bar{R}$) gives

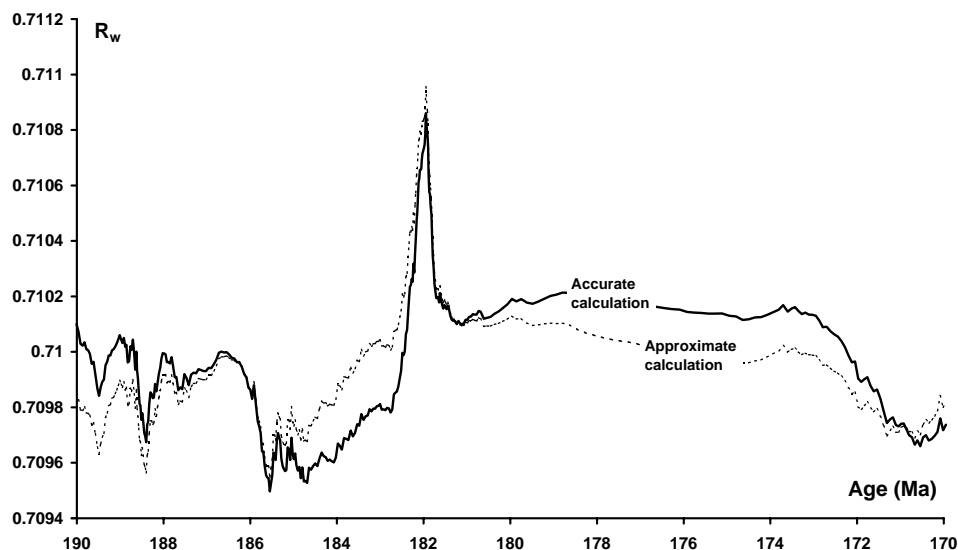


Fig. 7. Time-variation in weathering source $^{87}\text{Sr}/^{86}\text{Sr}$ ratio. Best-guess parameters from Table 1 have been used here together with Eq. (13) to give the accurate curve and Eq. (14) to give the approximate curve.

$$\Delta R_w = R_w - \overline{R_w} \approx \frac{\tau \dot{R}}{f_w}. \quad (14)$$

Note that the deviation from the mean is a scaled version of $\dot{R}(t)$ whatever values are chosen for the unknown constants and, hence, all $R_w(t)$ predictions will have a peak near 182 Ma. Eq. (14) is minimized using the smallest values of τ and $\overline{R_w}$ (from Table 1) along with a largest feasible f_w of 1.0. These values give $\Delta R_w = 0.00011$. Eq. (14), together with the appropriate mean value, also gives an approximate $R_w(t)$ curve which is shown in Fig. 7 for comparison with that derived from Eq. (12). This comparison supports the approximations used to produce Eq. (14) but note that calculation of $R_w(t)$ is always best done using Eq. (12).

Generalizing the above results to allow time-variation in any one of the source isotope ratios leads to the prediction that the deviation from the mean is well approximated by

$$\Delta R_x \approx \frac{\tau \dot{R}}{f_x}, \quad (15)$$

where x is w , h or d .

Hence, if the observed seawater $^{87}\text{Sr}/^{86}\text{Sr}$ time-variation is due to fluctuations in the $^{87}\text{Sr}/^{86}\text{Sr}$ ratio sourced from hydrothermal systems, Eq. (15) implies that a similar degree of variation is needed to that required for a weathering-ratio-variation explanation. In contrast, since the diagenetic source flux is an order of magnitude smaller than either the weathering or hydrothermal fluxes, a $R_d(t)$ explanation is very unlikely to be correct since Eq. (15) predicts very large variations of the order of 0.01.

6. Discussion

At this point we have examined the mutually exclusive hypotheses that the sharp rise in seawater $^{87}\text{Sr}/^{86}\text{Sr}$ value around 182 Ma was caused by a change in the weathering flux, a change in the hydrothermal flux, a change in the diagenetic flux, a change in the weathering source $^{87}\text{Sr}/^{86}\text{Sr}$ ratio, a change in the hydrothermal source $^{87}\text{Sr}/^{86}\text{Sr}$ ratio or a change in the diagenetic source $^{87}\text{Sr}/^{86}\text{Sr}$ ratio. In all cases, the conclusions are very similar. Each of these cases requires a short, sharp change in the parameter being considered at around 182 Ma. The precise size of this change depends upon the unknown, but constant, values assumed for the remaining parameters. However, values can be chosen which minimize the size of these changes thus giving a lower-bound to the size of the geological process responsible.

The most important conclusion from our analysis is that there is a genuine anomaly at 182 Ma which needs explaining. We can state, unequivocally, that there are no solutions to the seawater $^{87}\text{Sr}/^{86}\text{Sr}$ inversion problem in which there is no short-lived excursion at 182 Ma, in one of the source fluxes or one of the source $^{87}\text{Sr}/^{86}\text{Sr}$ values. We can only make this statement because we have shown that all unexplored solutions to the problem have a deviation from the mean which is simply a scaled version of the

time-derivative curve shown in Fig. 2. This emphasizes the point made at the start of this paper that this problem is under-constrained rather than unconstrained, i.e., it is possible to make definite statements about all solutions even though no single solution can be picked out. Note that the conclusion that a definite event occurred follows as soon as it is accepted that there is a short, sharp rise in the seawater $^{87}\text{Sr}/^{86}\text{Sr}$ curve at this time. The overall amount of rise is too large for it to be an artefact of data uncertainties and the time scale over which it occurred is short, compared to the oceanic residence time of strontium, even if this part of the section has significant dating errors. Thus, the Toarcian event is real and all that remains to be decided is whether it was a major or minor event.

In a little more detail, our analysis allows three of the possible explanations to be eliminated. Time-variations in the diagenetic flux or diagenetic isotope ratio would need to be unreasonably large if they are to account for the observed seawater $^{87}\text{Sr}/^{86}\text{Sr}$ fluctuations. In addition, an explanation in terms of time-variation in the hydrothermal flux seems improbable because of the lack of mechanisms for producing a short, sharp reduction in this flux. This leaves three potential explanations:

1. The rise in seawater $^{87}\text{Sr}/^{86}\text{Sr}$ ratio at around 182 Ma was caused by an increase in the strontium flux from continental weathering by the equivalent of at least 2% of the burial flux. Our best-guess is that this explanation actually requires an increase in the weathering flux by an amount equal to 20% of the burial flux.
2. The rise in seawater $^{87}\text{Sr}/^{86}\text{Sr}$ ratio at around 182 Ma was caused by an increase in the $^{87}\text{Sr}/^{86}\text{Sr}$ ratio of continental weathering products by at least 0.0001. Our best-guess is that this explanation actually requires an increase of about 0.0009.
3. The rise in seawater $^{87}\text{Sr}/^{86}\text{Sr}$ ratio at around 182 Ma was caused by an increase in the $^{87}\text{Sr}/^{86}\text{Sr}$ ratio from hydrothermal systems by at least 0.0001. Our best-guess is that this explanation actually requires an increase of about 0.0009.

Each of these three explanations appears to be feasible. The required increase in weathering flux is actually quite moderate whilst the required increases in isotope ratio are small compared to known variations in output from either weathering or hydrothermal sources.

A consequence of the fact that only moderate changes in parameters are needed is that a dramatic climatic deterioration as proposed by Pálffy and Smith (2000) is not necessary (although this does not mean that it did not happen). For example, if the 182 Ma event was caused by climate-induced fluctuations in the flux of weathered material from the continents then, with the best-guess scenario, a substantial increase in weathering is needed (20% of the burial flux) whereas, with the minimum deviation solution, the required increase in weathering flux drops tenfold. The minimum possible anomaly sizes are, however, strongly

affected by the values assumed for the seawater strontium residence time and for the peak slope in the seawater curve. Thus, the lower-bounds given in this paper may well be significantly revised upwards when future work, hopefully, provides improved estimates for these factors.

The above conclusions contrast sharply with those given in other recent publications concerning climatic changes at this time. Beerling et al. (2002) suggested that atmospheric $p\text{CO}_2$ levels increased by at least threefold with a minimum temperature increase of 3 °C, which has been supported more recently by McElwain et al. (2005). The belemnite $\delta^{18}\text{O}_{\text{carb}}$ record suggests an oceanic temperature increase of ~10 °C (McArthur et al., 2000; Jenkyns et al., 2002). A palaeotemperature increase of this magnitude would dramatically influence the hydrological cycle and enhance global weathering capabilities (Kump et al., 2000). This would have been exacerbated through the eruption and volcanic degassing of the Karoo–Ferrar continental flood basalts occurring at the same time (Encarnación et al., 1996; Duncan et al., 1997). However, recently published dates of the Karoo igneous province indicate that the duration of this igneous event was of the order of 8 Myr (Jourdon et al., 2005) and not a rapid pulse of igneous activity previously proposed (Encarnación et al., 1996; Duncan et al., 1997). Caution must be considered regarding the effect of continental flood basalts on CO_2 , as it has been recently documented that basalt weathering may in fact induce, in part, a CO_2 sink (Dessert et al., 2003).

More recently, Cohen et al. (2004) reported an $^{187}\text{Os}/^{188}\text{Os}$ excursion during the Toarcian OAE and suggest that the only likely mechanism to cause such an isotopic shift in osmium over a short time period (~100 kyr) is through a sudden increase in global weathering of the order of 400–800%. This is very different from the best-guess value of 20% reported in this paper. However, our 20% increase in weathering results from assuming that the steep rise in seawater strontium isotope ratio took approximately 1 Myr. If, in fact, it occurred much faster (i.e., over 100 kyr) then the corresponding gradient is higher by the same factor so that Eq. (11) now puts our best estimate of the increase at 200%. Moreover, if the gradient were ten times higher and, in addition, the weathering products were dominated by sedimentary rocks or young igneous material allowing riverine $^{87}\text{Sr}/^{86}\text{Sr}$ values to be as low as 0.708, Eq. (11) suggests a 650% increase in weathering flux at this time. Hence, on the basis of the results presented in this paper, we can only state that a major climatic event is not necessary to explain the observed excursion in the seawater $^{87}\text{Sr}/^{86}\text{Sr}$ curve during the Toarcian but we cannot rule out the possibility that one occurred.

On the other hand, it is worth noting that a 400% increase in global weathering rates would equate, using an average modern global denudation rate of ~48 mm/1000 years (Meybek, 1979), to a total global denudation rate of ~24 m of the Earth's surface during the 100 kyr of the $^{187}\text{Os}/^{188}\text{Os}$ excursion, which from our current understanding of sedimentation during the Early Toarcian would seem

unlikely. In addition, several mechanisms may produce a discrepancy between osmium and strontium for the Toarcian weathering event: (1) the $^{187}\text{Os}/^{188}\text{Os}$ curve has been generated from a single location within the northwest European sea-way; (2) the residence time of osmium is very short (<40 kyr) in comparison to strontium (Peucker-Ehrenbrink and Ravizza, 2000) and may reflect a localized effect; (3) diagenetic processes may influence the signal, as the high osmium ratios correspond with the rise and peak in sedimentary total organic carbon contents (Hesselbo et al., 2000).

A final point to make is that our assumption that a short, sharp event must result from a change in a single parameter is an idealization. In reality, some of the parameters may be strongly correlated. For example, climate change can cause a simultaneous alteration in the riverine flux and the strontium isotope ratio since warm conditions can, under the right circumstances, produce both higher continental erosion and higher strontium isotope ratios (Edmond, 1992; Edmond and Huh, 1997). Thus, if the weathering flux and weathering strontium isotope ratio changed together, the minimum 182 Ma excursions in these may be even smaller than the values given above.

7. Conclusion

This paper has shown that lower-bounds can be placed upon the variations in strontium source fluxes and isotope ratios responsible for observed fluctuations in the seawater $^{87}\text{Sr}/^{86}\text{Sr}$ curve. Thus, quantitative constraints can be applied to models of the causes of these fluctuations (e.g., enhanced weathering due to global climate change). When used to explain an abrupt increase in seawater $^{87}\text{Sr}/^{86}\text{Sr}$ ratio in the Early Jurassic, this approach demonstrates that a short, sharp event was responsible (i.e., it cannot be recreated by any models having slowly changing parameters). However, given current uncertainties in dating and in the strontium oceanic residence time, we cannot rule out the possibility that a fairly minor event was responsible rather than the major climatic event postulated by others.

Acknowledgments

We would like to thank two anonymous reviewers for their insightful comments.

Associate editor: Lee R. Kump

References

- Beerling, D.J., Lomas, M.R., Gröcke, D.R., 2002. On the nature of methane gas dissociation during the Toarcian and Aptian oceanic anoxic events. *Am. J. Sci.* **302**, 28–49.
- Berner, R.A., Rye, D.M., 1992. Calculation of the Phanerozoic strontium isotope record of the oceans from a carbon cycle model. *Am. J. Sci.* **292**, 136–148.
- Bralower, T.J., Fullagar, P.D., Paull, C.K., Dwyer, G.S., Leckie, R.M., 1997. Mid-Cretaceous strontium-isotope stratigraphy of deep-sea sections. *Geol. Soc. Am. Bull.* **109**, 1421–1442.

- Brass, G.W., 1976. The variation of the marine $^{87}\text{Sr}/^{86}\text{Sr}$ ratio during Phanerozoic time: interpretation using a flux model. *Geochim. Cosmochim. Acta* **40**, 721–730.
- Clemens, S.C., Farrell, J.W., Gromet, L.P., 1993. Synchronous changes in seawater strontium isotope composition and global climate. *Nature* **363**, 607–610.
- Cohen, A.S., Coe, A.L., Harding, S.L., Schwark, L., 2004. Osmium isotope evidence for the regulation of atmospheric CO_2 by continental weathering. *Geology* **32**, 157–160.
- Crame, J.A., McArthur, J.M., Pirrie, D., Riding, J.B., 1999. Strontium isotope correlation of the basal Maastrichtian stage in Antarctica to the European and US biostratigraphic schemes. *J. Geol. Soc. London* **156**, 957–964.
- Dessert, C., Dupré, B., Gaillardet, J., François, L.M., Allègre, C.J., 2003. Basalt weathering laws and the impact of basalt weathering on the global carbon cycle. *Chem. Geol.* **202**, 257–273.
- DePaolo, D.J., Ingram, B.L., 1985. High-resolution stratigraphy with strontium isotopes. *Science* **227**, 938–941.
- Duncan, R.A., Hooper, P.R., Rehacek, J., Marsh, J.S., Duncan, A.R., 1997. The timing and duration of the Karoo igneous event, southern Gondwana. *J. Geophys. Res.* **102**, 18127–18138.
- Edmond, J.M., 1992. Himalayan tectonics, weathering processes and the strontium isotope record in marine limestones. *Science* **258**, 1594–1597.
- Edmond, J.M., Huh, Y., 1997. Chemical weathering yields from basement and orogenic terrains in hot and cold climates. In: Ruddiman, W.F. (Ed.), *Tectonic Uplift and Climate Change*. Plenum Press, New York, pp. 329–351.
- Encarnación, J., Fleming, T.H., Elliot, D.H., Eales, H.V., 1996. Synchronous emplacement of Ferrar and Karoo dolerites and the early breakup of Gondwana. *Geology* **24**, 535–538.
- Françoise, L.M., Walker, J.C.G., 1992. Modelling the Phanerozoic carbon cycle and climate: Constraints from the $^{87}\text{Sr}/^{86}\text{Sr}$ isotopic ratio of seawater. *Am. J. Sci.* **292**, 81–135.
- Gröcke, D.R., Price, G.D., Ruffell, A.H., Mutterlose, J., Baraboshkin, E., 2003. Isotopic evidence for Late Jurassic–Early Cretaceous climate change. *Palaeogeogr. Palaeoclim. Palaeoecol.* **202**, 97–118.
- Hall, R.L., McNicoll, V., Gröcke, D.R., Craig, J., Johnston, K., 2004. Integrated stratigraphy in the lower and middle Fernie Formation in Alberta and British Columbia, western Canada. *Revista Italiana di Paleontologia e Stratigrafia* **110**, 61–68.
- Hesselbo, S.P., Gröcke, D.R., Jenkyns, H.C., Bjerrum, C., Farrimond, P., Morgans Bell, H., Green, O., 2000. Methane hydrate dissociation during a Jurassic oceanic anoxic event. *Nature* **406**, 392–395.
- Hesselbo, S.P., Meister, C., Gröcke, D.R., 2002. A potential global stratotype for the Sinemurian–Pliensbachian boundary (Lower Jurassic), Robin Hood's Bay, UK: ammonite faunas and isotope stratigraphy. *Geol. Mag.* **137**, 601–607.
- Hodell, D.A., Mead, G.A., Mueller, P.A., 1990. Variation in the strontium isotopic composition of seawater (8 Ma to present): Implications for chemical weathering rates and dissolved fluxes to the oceans. *Chem. Geol.* **80**, 291–307.
- Hodell, D.A., Mueller, P.A., Garrido, J.R., 1991. Variations in the strontium isotopic composition of seawater during the Neogene. *Geology* **19**, 24–27.
- Hodell, D.A., Mueller, P.A., McKenzie, J.A., Mead, G.A., 1989. Strontium isotope stratigraphy and geochemistry of the late Neogene ocean. *Earth Planet. Sci. Lett.* **92**, 165–178.
- Jenkyns, H.C., Paull, C.K., Cummins, D.I., Fullagar, P.D., 1995. Strontium isotope stratigraphy of lower Cretaceous atoll carbonates in the mid-Pacific Mountains. *Proc. Ocean Drill. Prog. Sci. Res.* **143**, 89–97.
- Jenkyns, H.C., Jones, C.E., Gröcke, D.R., Hesselbo, S.P., Parkinson, D.N., 2002. Chemostratigraphy in the Jurassic: applications, limitations and implications for palaeoceanography. *J. Geol. Soc. London* **159**, 351–378.
- Jones, C.E., 1992. Strontium isotopes in Jurassic and Early Cretaceous seawater. D.Phil. Thesis, University of Oxford, England.
- Jones, C.E., Jenkyns, H.C., 2001. Seawater strontium isotopes, oceanic anoxic events, and seafloor hydrothermal activity in the Jurassic and Cretaceous. *Am. J. Sci.* **301**, 112–149.
- Jones, C.E., Jenkyns, H.C., Coe, A.L., Hesselbo, S.P., 1994a. Strontium isotopic variations in Jurassic and Cretaceous seawater. *Geochim. Cosmochim. Acta* **58**, 3061–3074.
- Jones, C.E., Jenkyns, H.C., Hesselbo, S.P., 1994b. Strontium isotopes in Early Jurassic seawater. *Geochim. Cosmochim. Acta* **58**, 1285–1301.
- Jourdon, F., Féraud, G., Bertrand, H., Kampunzu, A.B., Tshoso, G., Watkeys, M.K., Gall, B.L., 2005. Karoo large igneous province: brevity, origin, and relation to mass extinction questioned by new $^{40}\text{Ar}/^{39}\text{Ar}$ age data. *Geology* **33**, 745–748.
- Koepnick, R.B., Burke, W.H., Denison, R.E., Hetherington, E.A., Nelson, H.F., Otto, J.B., Waite, L.E., 1985. Construction of the seawater $^{87}\text{Sr}/^{86}\text{Sr}$ curve for the Cenozoic and Cretaceous: supporting data. *Chem. Geol.* **58**, 55–81.
- Koepnick, R.B., Denison, R.E., Burke, W.H., Hetherington, E.A., Dahl, D.A., 1990. Construction of the Triassic and Jurassic portion of the Phanerozoic curve of seawater $^{87}\text{Sr}/^{86}\text{Sr}$. *Chem. Geol.* **80**, 327–349.
- Kump, L.R., Brantley, S.L., Arthur, M.A., 2000. Chemical, weathering, atmospheric CO_2 , and climate. *Ann. Rev. Earth Planet Sci.* **28**, 611–667.
- Martin, E.E., Shackleton, N.J., Zachos, J.C., Flower, B.P., 1999. Orbitally-tuned Sr isotope chemostratigraphy for the late middle to late Miocene. *Paleoceanography* **14**, 74–83.
- McArthur, J.M., Donovan, D.T., Thirlwall, M.F., Fouke, B.W., Matthey, D., 2000. Strontium isotope stratigraphy of the Oceanic Anoxic Event, Early Toarcian (Jurassic). *Earth Planet. Sci. Lett.* **179**, 269–285.
- McArthur, J.M., Kennedy, W.J., Chen, M., Thirlwall, M.F., Gale, A.S., 1994. Strontium isotope stratigraphy for Late Cretaceous time: direct numerical calibration of the Sr isotope curve based on the US Western Interior. *Palaeogeogr. Palaeoclim. Palaeoecol.* **108**, 95–119.
- McArthur, J.M., Kennedy, W.J., Gale, A.S., Thirlwall, M.F., Chen, M., Burnett, J., Hancock, J.M., 1992. Strontium isotope stratigraphy in the Late Cretaceous: intercontinental correlation of the Campanian/Maastrichtian boundary. *Terra Nova* **4**, 385–393.
- McArthur, J.M., Thirlwall, M.F., Chen, M., Gale, A.S., Kennedy, W.J., 1993. Strontium isotope stratigraphy in the late Cretaceous: numerical calibration of the Sr isotope curve and intercontinental correlation for the Campanian. *Paleoceanography* **8**, 859–873.
- McArthur, J.M., Howarth, R.J., Bailey, T.R., 2001. Strontium isotope stratigraphy: LOWESS Version 3. Best-fit line to the marine Sr-isotope curve for 0–509 Ma and accompanying look-up table for deriving numerical age. *J. Geol.* **109**, 155–169.
- McCauley, S.E., DePaolo, D.J., 1997. The marine $^{87}\text{Sr}/^{86}\text{Sr}$ and $\delta^{18}\text{O}$ records, Himalayan alkalinity fluxes and Cenozoic climate models. In: Ruddiman, W.F. (Ed.), *Tectonic Uplift and Climate Change*. Plenum Press, New York, pp. 427–455.
- McElwain, J.C., Wade-Murphy, J., Hesselbo, S.P., 2005. Changes in carbon dioxide during an oceanic anoxic event linked to intrusion into Gondwana coals. *Nature* **435**, 479–482.
- McLaughlin, M., McArthur, J.M., Thirlwall, M.F., Howarth, R., Burnett, J., Gale, A.S., Kennedy, W.J., 1995. Sr isotope evolution of Maastrichtian seawater, determined from the chalk of Hemmoor, NW Germany. *Terra Nova* **7**, 491–499.
- Meybek, M., 1979. Concentratio des eaux fluviales en elements najeurs et apports en solution aux oceans. *Rev. Geol. Dyn. Geogr. Phys.* **21**, 215–246.
- Oslick, J.S., Miller, K.G., Feigenson, M.D., 1994. Oligocene–Miocene strontium isotopes: stratigraphic revisions and correlations to an inferred glacioeustatic record. *Paleoceanography* **9**, 427–443.
- Pálffy, J., Smith, P.L., 2000. Synchrony between Early Jurassic extinction, oceanic anoxic event and the Karoo–Ferrar flood basalt volcanism. *Geology* **28**, 747–750.
- Palmer, M.R., Edmond, J.M., 1989. The strontium isotope budget of the modern ocean. *Earth Planet. Sci. Lett.* **92**, 11–26.
- Palmer, M.R., Elderfield, H., 1985. Sr isotope composition of seawater over the past 75 Myr. *Nature* **314**, 526–528.

- Peucker-Ehrenbrink, B., Ravizza, G., 2000. The marine osmium isotope record. *Terra Nova* **12**, 205–219.
- Podlaha, O.G., Mutterlose, J., Veizer, J., 1998. Preservation of $\delta^{18}\text{O}$ and $\delta^{13}\text{C}$ in belemnite rostra from the Jurassic/Early Cretaceous successions. *Am. J. Sci.* **298**, 324–347.
- Price, G.D., Gröcke, D.R., 2002. Strontium-isotope stratigraphy and oxygen- and carbon-isotope variation during the Middle Jurassic–Early Cretaceous of the Falkland Plateau, South Atlantic. *Palaeogeogr. Palaeoclim. Palaeoecol.* **183**, 209–222.
- Sugarman, P.J., McCartan, L., Miller, K.G., Feigenson, M.D., Pekar, S., Kistler, R.W., Robinson, A.G., 1997. Strontium-isotopic correlation of Oligocene to Miocene sequences, New Jersey and Florida. *Proc. Ocean Drill. Prog. Sci. Res.* **150**, 147–159.
- Veizer, J., Buhl, D., Diener, A., Ebner, S., Podlaha, O.G., Bruckschen, P., Jasper, T., Korte, C., Schaaf, M., Ala, D., Azmy, K., 1997. Strontium isotope stratigraphy: potential resolution and event correlation. *Palaeogeogr. Palaeoclim. Palaeoecol.* **132**, 65–77.
- Veizer, J., Ala, D., Azmy, K., et al., 1999. $^{87}\text{Sr}/^{86}\text{Sr}$, ^{13}C and ^{18}O evolution of Phanerozoic seawater. *Chem. Geol.* **161**, 59–88.
- Wallmann, K., 2001. Controls on the Cretaceous and Cenozoic evolution of seawater composition, atmospheric CO_2 and climate. *Geochim. Cosmochim. Acta* **65**, 3005–3025.